Molecular Therapy
Oncolytics
Original Article

LINC01296 promotes neuroblastoma tumorigenesis via the NCL-SOX11 regulatory complex

Jing Wang,[1,3] Zuopeng Wang,[1,3] Weihong Lin,[1] Qilei Han,[1] Hanlei Yan,[1] Wei Yao,[1] Rui Dong,[1] Deshui Jia,[2] Kuiran Dong,[1] and Kai Li[1]

[1]Department of Pediatric Surgery, Children's Hospital of Fudan University, National Children's Medical Center, 399 Wanyuan Road, Shanghai 201102, China; [2]Laboratory of Cancer Genomics and Biology, Department of Urology, and Institute of Translational Medicine, Shanghai General Hospital, Shanghai Jiao Tong University School of Medicine, Shanghai 200080, China

Neuroblastoma (NB) is the most common extracranial solid tumor in childhood. Long non-coding RNA LINC01296 has been shown to predict the invasiveness and poor outcomes of patients with NB. Our study validated its prognostic value and investigated the biological function and potential mechanism of LINC01296 regulating NB. Results illuminated that LINC01296 expression was significantly correlated with unfavorable prognosis and malignant clinical features according to the public NB database. We identified that silencing LINC01296 repressed NB cell proliferation and migration and promoted apoptosis. Moreover, LINC01296 knockdown inhibited tumor growth *in vivo*. The opposite results were observed through the dCas9 Synergistic Activation Mediator System (dCas9/SAM) activating LINC01296. Mechanistically, we revealed that LINC01296 could directly bind to nucleolin (NCL), forming a complex that activated SRY-box transcription factor 11 (SOX11) gene transcription and accelerated tumor progression. In conclusion, our findings uncover a crucial role of the LINC01296-NCL-SOX11 complex in NB tumorigenesis and may serve as a prognostic biomarker and effective therapeutic target for NB.

INTRODUCTION

Neuroblastoma (NB) is a type of embryonic malignant solid tumor originating from neural crest cells, which is the most common abdominal malignant tumor in children.[1,2] Due to its rapid progress and high malignancy, the prognosis of patients with advanced NB is always unsatisfactory, with a 5-year overall survival rate of 30%–40%.[3,4] Therefore, it is necessary to understand the molecular mechanism of NB and develop novel therapeutic targets for NB.

Long non-coding RNA (lncRNA) is longer than 200 nucleotides in length with no protein-coding function.[5] Recent studies have shown that lncRNA plays a crucial role in the process of cell differentiation, cell growth, cell migration, and tumorigenesis.[6,7] lncRNA has been reported to regulate gene expression in cancers through chromatin modification and remodeling, target gene transcription, post-translational modification, and interacting with RNA-binding proteins (RBPs).[7,8] Nucleic acid drugs targeting lncRNAs, including antisense oligonucleotide (ASO), locked nucleic acid (LNA), and nanoparticle-short interfering RNA (Nano-siRNA),[9] have been used in pre-clinical or clinical trials for several cancers, such as breast cancer and NB.[9–12] Similar to several other tumors, lncRNA also has an essential effect on the occurrence and development of NB, and can serve as a biomarker for early diagnosis and predicting the prognosis.[13] For example, sense-antisense lncRNA pair cancer susceptibility 15 (CASC15) and NB-associated transcript 1 (NBAT-1) determines the susceptibility of NB through the USP36-CHD7-SOX9 regulatory axis, and both CASC15 and NBAT-1 can be used as independent risk factors for the prognosis of NB.[14–16]

Our previous study identified that lncRNA LINC01296 was significantly upregulated in advanced-stage tumors compared with early-stage tumors and could predict the invasive clinical features and poor outcomes of patients with NB.[17] In this study, we found that LINC01296 enhanced cell proliferation, cell migration, and repressed cell apoptosis in NB. Mechanistically, RBP nucleolin (NCL) bound with LINC01296 to form a complex that could interact with the promoter of oncogene SOX11 and activate its transcription. Our findings demonstrated that LINC01296 played a vital role in the tumor progression of NB, and the LINC01296/NCL/SOX11 complex could serve as a novel therapeutic target for NB.

Received 23 September 2021; accepted 3 February 2022;
https://doi.org/10.1016/j.omto.2022.02.007.

[3]These authors contributed equally

Correspondence: Deshui Jia, Laboratory of Cancer Genomics and Biology, Department of Urology, and Institute of Translational Medicine, Shanghai General Hospital, Shanghai Jiao Tong University School of Medicine, Shanghai 200080, P.R. China.
E-mail: deshui.jia@shgh.cn
Correspondence: Kuiran Dong, Department of Pediatric Surgery, Children's Hospital of Fudan University, National Children's Medical Center, 399 Wanyuan Road, Shanghai 201102, P.R. China.
E-mail: kuirand@hotmail.com
Correspondence: Kai Li, Department of Pediatric Surgery, Children's Hospital of Fudan University, National Children's Medical Center, 399 Wanyuan Road, Shanghai 201102, P.R. China.
E-mail: likai2727@163.com

RESULTS

LINC01296 serves as a potential prognostic biomarker in NB

Our previous study revealed that LINC01296 was associated with malignant clinical characteristics in 28 primary NB tumor tissues in our hospital. To further validate this association in a larger sample size, we used R2: Genomic Analysis and Visualization Platform (http://r2.amc.nl). In a dataset containing 88 patients with NB (Tumor Neuroblastoma public - Versteeg - 88 - MAS5.0 - u133p2), the expression levels of LINC01296 were positively correlated with the International Neuroblastoma Staging System (INSS) stage (Figure 1A). Patients with MYCN proto-oncogene (MYCN) amplification and patients diagnosed after 18 months of age usually have higher LINC01296 expression levels (Figures 1B and 1C). Moreover, high LINC01296 expression was significantly correlated with tumor recurrence, progression, and death, but not gender (Figures 1D–1F). As expected, patients with elevated LINC01296 expression had poor overall survival probabilities and event-free survival probabilities (Figures 1G and 1H). These clinical data indicated that the LINC01296 serves as a crucial biomarker for outcomes in patients with NB and that targeting LINC01296 may be an effective therapeutic strategy.

LINC01296 promotes an invasive tumor phenotype in NB cells

To investigate the function of LINC01296 in cells, we used small hairpin RNA (shRNA) to knock down LINC01296 and an RNA-guided CRISPR activation system, the dCas9 Synergistic Activation Mediator System (dCas9/SAM) to activate LINC01296 expression in NB cells endogenously. The expression level of LINC01296 was relatively higher in SK-N-BE(2)C and SK-N-SH and lowered in SK-N-AS (Figure S1A). Thus, SK-N-BE(2)C and SK-N-SH were chosen for developing knockdown cells, and SK-N-BE(2)C and SK-N-AS were selected for constructing dCas9/SAM cells for subsequent study. shLINC01296 remarkably suppressed LINC01296 in NB cells (Figures 2A and S1B). The reduction of LINC01296 resulted in decreased proliferation according to the Cell Counting Kit-8 (CCK-8) growth curve (Figure 2B). Consistently, LINC01296 knockdown (KD) led to impaired clonogenic ability in the colony formation assay (Figures 2C and 2D) and significantly reduced the proportion of 5-ethynyl-2′-deoxyuridine-positive (EdU^+) cells in the KD cells (Figures 2E and 2F). LINC01296 KD also significantly decreased the cell migration (Figures 2G and 2H) but enhanced the apoptosis of NB cells (Figures 2I and 2J). Western blot of apoptosis markers, including poly-ADP ribose polymerase (PARP), cleaved PARP, caspase-3, and cleaved caspase-3, confirmed this result (Figure 2K).

For the overexpression of LINC01296, we used the dCas9/SAM transcriptional activation system to activate LINC01296 expression. We established three guide RNAs targeting the promoter region of LINC01296 (single-guide [sg]LINC01296) and co-expressed with dCas9-VP64 and MS2-P65-HSF1 plasmids into SK-N-BE(2)C and SK-N-AS cells, which could assemble the SAM complex to the promoter region of LINC01296 and transcriptionally activate its expression.[18] The guide RNAs enhanced LINC01296 expression (Figures 3A and S1C), and we chose the sgRNA with the highest efficacy for the follow-up experiment (sg2). Consistent with the results mentioned above, the CCK-8 assay (Figure 3B), the colony formation assay (Figures 3C and 3D), and the EdU assay (Figures 3E and 3F) showed increased proliferation in sgLINC01296 cells. Similarly, the result of the transwell assay revealed enhanced cell migration in sgLINC01296 groups (Figures 3G and 3H). Furthermore, the flow cytometry showed decreased apoptosis cells compared to control cells (Figures 3I and 3J). In addition, western blot analysis provided us with evidence that the overexpression of LINC01296 could reduce the expression level of PARP and caspase-3 but upregulate the expression level of cleaved PARP and cleaved caspase-3 (Figure 3K).

In addition, we found decreased xenograft tumor growth with LINC01296-KD SK-N-BE(2)C cells (Figures 4A–4C) and increased tumor volume in xenografts with LINC01296 activation SK-N-AS cells (Figures 4D–4F). Furthermore, the immunohistochemistry (IHC) staining showed a lower expression of Ki-67 in LINC01296-KD tumor tissues than the control group, and the contrary result was observed in LINC01296 activation tumor tissues (Figures 4G and 4H), which was consistent with our *in vitro* data. Collectively, these results confirmed that LINC01296 is an oncogene in NB, and it promoted tumor proliferation *in vitro* and *in vivo*.

LINC01296 directly binds to NCL

The function of lncRNAs is closely related to their subcellular localization.[19] Thus, we separated the cytoplasmic and nuclear RNA components of SK-N-BE (2)C and SK-N-SH cells. qRT-PCR (polymerase chain reaction) was carried out to measure the expression ratio of LINC01296 in the nucleus and cytoplasm. LINC01296 was mainly located in the nuclei of NB cells (Figure 5A). RNA fluorescence *in situ* hybridization (FISH) also confirmed the localization of LINC01296 in nuclei (Figures 5B and S1). One of the most critical functions of lncRNAs located in the nucleus is that they interact with specific proteins to regulate the expression of target genes.[20] Therefore, we used biotinylated LINC01296 probes to perform chromatin isolation by RNA purification (ChIRP) assays coupled with mass spectrometry (MS) in SK-N-BE(2)C cells to explore proteins specifically binding with LINC01296. Nineteen proteins were identified by MS (Figure 5C; Table S7). Among these 19 proteins, NCL was similarly enriched in the nuclei with a higher binding score. LIN01296 was predicted to interact with NCL with high interaction probabilities using RPISeq (http://pridb.gdcb.iastate.edu/RPISeq/references.php) (Table S8). Then, to confirm this interaction relationship, we conducted the RNA immunoprecipitation (RIP) assay in SK-N-BE(2)C and SK-N-SH cells. qRT-PCR analyses of purified RNA from IP confirmed that LINC01296 was significantly enriched in anti-NCL antibody compared to immunoglobulin G (IgG) (Figures 5D and 5E). These results demonstrated that LINC01296 specifically interacts with NCL in NB cells.

NCL acts as an oncogene to promote NB progression

Previous studies have reported that NCL is involved in cell proliferation, angiogenesis, apoptosis regulation, stress response, and microRNA

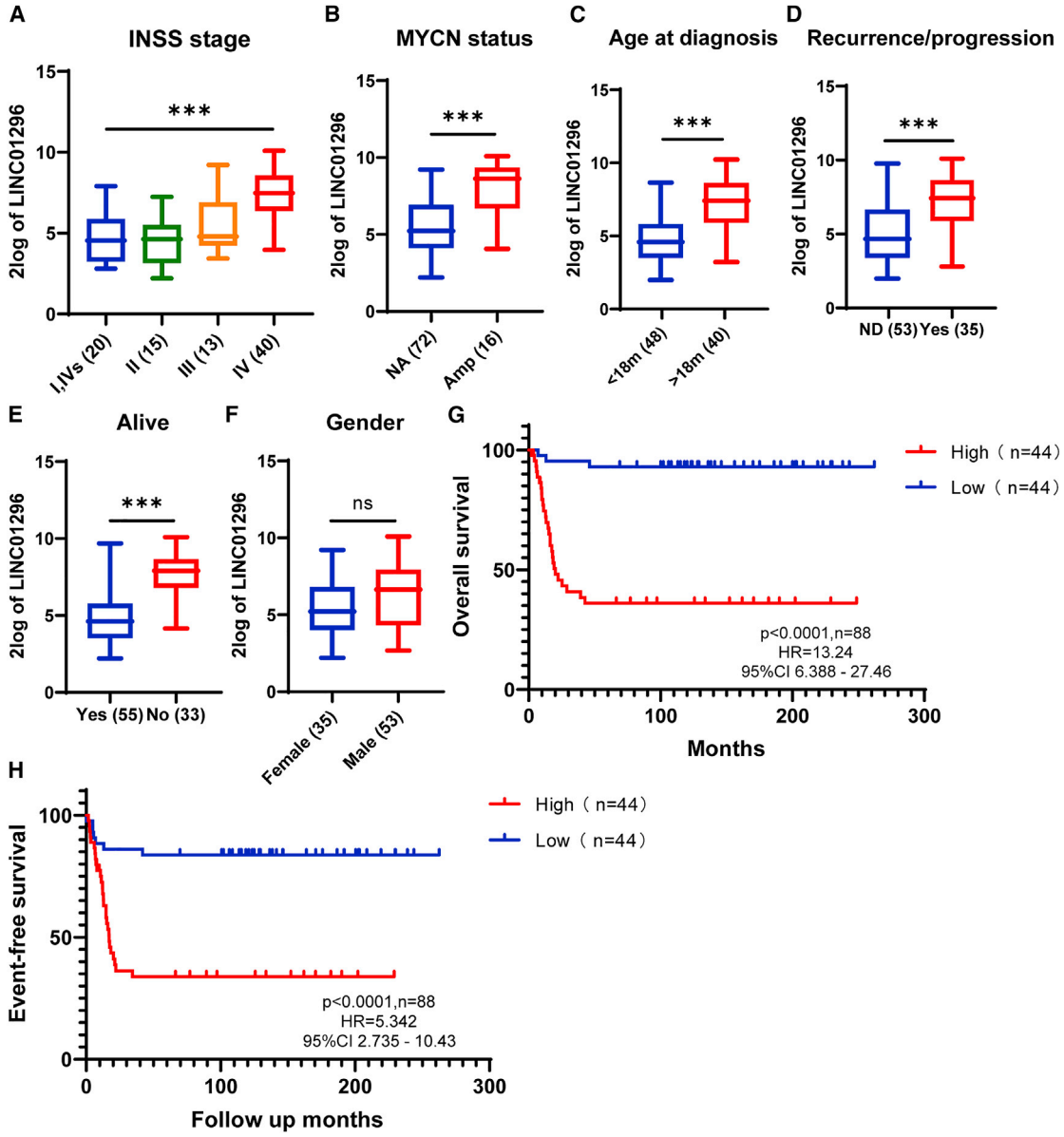

Figure 1. LINC01296 is a prognostic biomarker in neuroblastoma (NB)

(A) Relative expression of LINC01296 was correlated with the INSS stage. One-way ANOVA test was performed for all of the groups. (B) Relative expression of LINC01296 in MYCN-amplified tumor and non-amplified tumor. Amp, MYCN amplification; NA, MYCN non-amplification. (C) Relative expression of LINC01296 in different diagnostic age groups. <18m, less than 18 months; >18m, more than 18 months. (D) Relative expression of LINC01296 in patients with or without disease recurrence or progression. ND, no disease. (E) Relative expression of LINC01296 in patients alive or dead. (F) Relative expression of LINC01296 in males and females. (G and H) Kaplan-Meier curves of overall survival (OS) and event-free survival (EFS) of patients with high and low LINC01296 expression. The cutoff for high and low LINC01296 expression was 5.73 (log2 of raw expression values), according to the median of the LINC01296 expression levels of 88 patients in the cohort. *p < 0.05; **p < 0.01; ***p < 0.001; ns, not significant.

processing in cancer.[21,22] We found that NCL is significantly correlated with LINC01296 in public database R2: Genomics Analysis and Visualization Platform (R = 0.2325, p = 0.0293, n = 88; Figure 5F). Moreover, the database results showed that higher NCL expression levels were associated with poorer survival rates (Figures 5G and 5H). Consistently, KD of NCL in SK-N-BE(2)C and SK-N-SH cells (Figure 6A) significantly inhibited NB cell growth, colony formation ability (Figures 6B, 6C, and 6E), and cell migration ability (Figures 6D and 6F) and stimulated cell apoptosis (Figures 6G and 6H). Thus, NCL may function as an oncogene to promote NB progression.

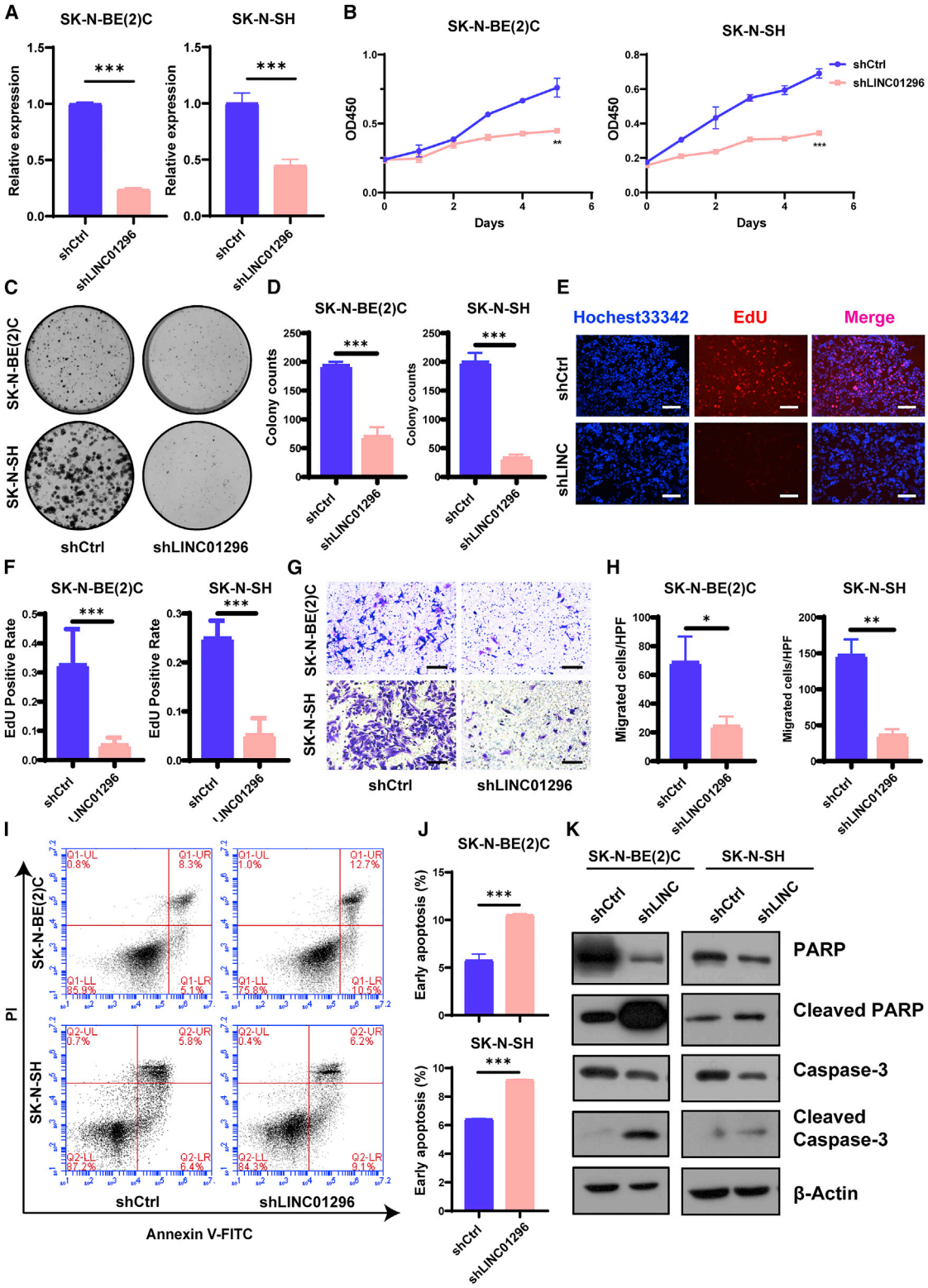

(legend on next page)

LINC01296 regulates SOX11 through transcriptional activation

Since LINC01296 is predominantly located in the nuclei of NB cells, we performed ChIRP-seq to identify the potential DNA binding loci of LINC01296 in SK-N-BE(2)C cells. A total of 3,055 peaks of the gene promoter regions that LINC01296 could bind were detected (Figures S2A and S2B). Gene Ontology (GO) analysis of identified genes showed enrichment in items of cellular metabolic process, generation of neurons, and neurogenesis (Figures 7A and S2D), and Kyoto Encyclopedia of Genes and Genomes (KEGG) pathway analysis revealed enrichment in epidermal growth factor receptor (EGFR) tyrosine kinase inhibitor resistance and the ErbB signaling pathway (Figure S2C), which conforms to the role of LINC01296 in cell proliferation. ChIRP-qPCR further validated 15 genes involved in these items, and 6 (BCL2, MAP2K2, SOX11, BRD4, LMO3, SMARCA1) of these genes were significantly enriched in the LINC01296 probe compared to controls (Figure 7B). Most of these genes have been reported to regulate malignancy tumorigenesis or progression.[23–28] In addition, the mRNA expression levels of these genes were confirmed by qRT-PCR. The transcript levels of BCL2, SOX11, BRD4, LMO3, and SMARCA1 were significantly reduced with LINC01296-KD (Figure 7C). We then referred to the database R2: Genomics Analysis and Visualization Platform. We found positive correlations between LINC01296 and SOX11 ($r = 0.464$, $p < 0.001$), BRD4 ($r = 0.228$, $p < 0.001$), and LMO3 ($r = 0.413$, $p < 0.001$) in clinical NB tumor samples according to the dataset Tumor Neuroblastoma public - Versteeg - 88 - MAS5.0 - u133p2 ($n = 88$) (Figure 7D). Increased SOX11 expression was associated with decreased overall survival in the dataset Tumor Neuroblastoma public - Versteeg - 88 - MAS5.0 - u133p2 ($n = 88$) and Tumor Neuroblastoma SEQC - 498 - custom ($n = 496$) (Figures S3A and S3B). Consistent with the clinical association, SOX11 levels were significantly decreased in the LINC01296-KD cells, determined by qRT-PCR and immunoblotting, and the level of SOX11 protein was markedly increased in the LINC01296 overexpression cells by the dCas9/SAM system (Figures 7E and 7F). The downregulated SOX11 in the LINC01296-KD group and elevated SOX11 in the LINC01296 overexpression group of xenograft tumors were also detected by immunoblotting (Figures S3C and S3D). The result of ChIRP-seq showed that LINC01296 was bound to the SOX11 promoter (chr2:5,833,818-5,834,778), with a length of 961 bp. We constructed a luciferase reporter vector to validate this interaction by fusing the binding region in SOX11 promoter sequences detected by ChIRP. The overexpression of LINC01296 resulted in increased reporter luciferase activity (Figure 7G).

A previous study has revealed that SOX11 plays a role in cell growth and proliferation and controls chromatin accessibility in NB.[29] Similarly, cell proliferation and migration ability were significantly increased in SOX11 overexpressed SK-N-BE(2)C cells (Figures S3C–S3F). Furthermore, the overexpression of SOX11 could rescue the reduced cell proliferation, migration, and promoted cell apoptosis due to LINC01296-KD (Figures 7H–7O and S4A–S4E). These findings collectively demonstrated that LINC01296 bound to SOX11 promoter and activated its expression.

LINC01296-NCL complex regulating NB progression through SOX11

As NCL bound with LINC01296 to form an RNA-protein complex, we wondered whether NCL could also regulate SOX11. Western blot analysis showed an apparent reduction of SOX11 protein after the ablation of NCL (Figure S4F). Then, we designed qPCR primers targeting two DNA regions in the SOX11 promoter region detected by ChIRP. The ChIP-qPCR assay that was conducted validated that NCL interacted with the SOX11 promoter compared to IgG control by both primers in SK-N-BE(2)C and SK-N-SH cells (Figure 7P). Taken together, these results indicated that NCL and LINC01296 could collaboratively upregulate the expression of SOX11 in NB cells.

DISCUSSION

Through the lncRNA microarray of advanced-stage tumor samples compared to early-stage tumor samples, we identified LINC01296 as the most enriched lncRNA in advanced-stage cases with a fold change of 13.96. It was noticed that LINC01296 expression levels were positively correlated with known risk factors for NB, including age at diagnosis, INSS stage, risk groups, MYCN status, serum lactate dehydrogenase (LDH), and serum neuron-specific enolase (NSE) in 28 cases.[17] We also found that the high expression levels of LINC01296 in NB patients were positively correlated with advanced INSS stage, MYCN amplification and patients diagnosed after 18 months, tumor recurrence or progression, and tumor death according to the NB public database, which had a larger sample size of 88 patients. Furthermore, elevated LINC01296 was significantly associated with poor overall survival probabilities and event-free survival probabilities. Therefore, LINC01296 may serve as a prognostic biomarker for NB. Similarly, LINC01296 could predict poor clinical prognosis of gastric cancer,[30] breast cancer,[31] colorectal cancer,[32] and non-small cell lung cancer (NSCLC),[33] indicating the predictive value of LINC01296 as a prognostic biomarker in tumors. To investigate the role of LINC01296 in NB, we used shRNA to knock down its expression and used the dCas9/SAM system to activate its transcription in NB cells endogenously. Cell proliferation and migration ability were inhibited and cell apoptosis was increased after knocking down LINC01296. The

Figure 2. Knockdown of LINC01296 inhibits NB cell proliferation and migration and promotes apoptosis *in vitro*

(A) qRT-PCR detected the efficiency of LINC01296 knockdown in SK-N-BE(2)C and SK-N-SH cells. (B) CCK-8 assay showed reduced cell viability of NB cells after LINC01296 knockdown. Student's t-test was performed on day 5 for 2 groups. (C and D) Colony formation assay showed the decreased clonogenic ability of NB cells after LINC01296 knockdown. (E and F) EdU assay showed a significantly reduced the proportion of EdU^+ cells in the LINC01296 knockdown SK-N-BE(2)C cells. Scale bar, 100 μm. (G and H) Transwell assay showed decreased cell migration ability in LINC01296 knockdown cells after incubation for 24 h. Scale bar, 50 μm. HPF, high-power field. (I and J) Flow cytometry analysis detected enhanced apoptosis of shLINC01296 NB cells. (K) Western blot experiment detected the PARP, cleaved PARP, caspase-3, and cleaved caspase-3 protein expression in shCtrl (control) and shLINC01296 NB cells.

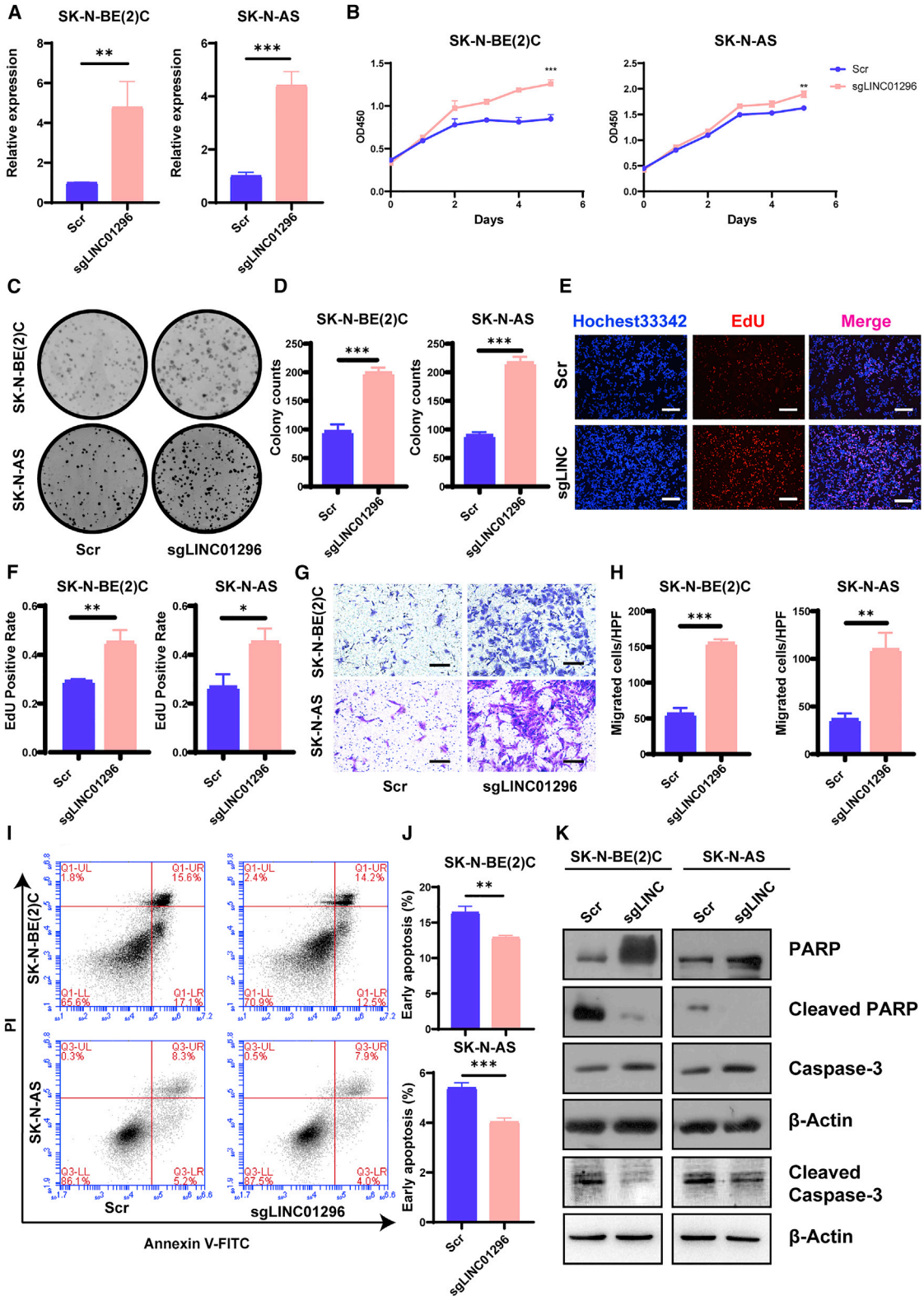

(legend on next page)

xenograft tumor growth assay showed the same thing, which is in keeping with studies of other tumors.[30–33] For instance, LINC01296 (also known as LNMAT1) epigenetically activates C-C motif chemokine ligand 2 (CCL2) expression by recruiting hnRNPL to the CCL2 promoter, promoting lymphatic metastasis of bladder cancer.[34] In NSCLC, LINC01296 (also known as DUXAP9-206) induces cell proliferation and cell metastasis by interacting with Cbl-b, decreasing the degradation of the EGFR and reinforcing EGFR signaling,[35] indicating an oncogene role of LINC01296 in several kinds of tumors.

Recent studies revealed that lncRNA could regulate gene expression through multiple mechanisms, including by recruiting transcription factors to DNA targets, by forming heterogeneous ribonucleoprotein (hnRNP) complexes, and by acting as a decoy to bind RBP and microRNA, or directly interacting with RNA and DNA through base pairing.[19] The regulating mechanism of lncRNA is closely related to its subcellular localization.[36] Since LINC01296 is mainly located at nuclear, we speculated that the function of LINC01296 may be to bind with RBP and DNA. Thus, we performed ChIRP-liquid chromatography (LC)/MS and ChIRP-seq and found that LINC01296 has interacted with NCL protein and the SOX11 gene promoter. NCL is one of the most abundant proteins in the nucleolus and is involved in various biological aspects, including chromatin remodeling, pre-RNA maturation, rDNA transcription, ribosome assembly, tumor cell proliferation, survival, and apoptosis.[21] A previous study reported that NCL could upregulate vascular endothelial growth factor (VEGF) expression by binding to the G- and C-rich sequences of the VEGF gene promoter and promote tumor angiogenesis.[37] In colon cancer, NCL could combine with lncRNA CYTOR to form a complex, activating the nuclear factor κB (NF-κB) pathway and the epithelial-mesenchymal transition (EMT) process to enhance tumor cell proliferation, migration, and invasion.[38] In the study of NB, *in vitro* data have confirmed that NCL maintains the stemness of NB cancer stem cells by binding to the CD34 gene promoter region to activate its transcription and can be used as a functional target of a novel antitumor stem cell drug salinomycin.[39] Here, we identified that LINC01296 could be precipitated by the anti-NCL antibody through the RIP assay, confirming the binding relationship between LINC01296 and NCL. The KD of NCL decreased cell proliferation and migration ability and enhanced the cell apoptosis of NB cells. Identically, elevated levels of NCL were associated with the unfavorable prognosis of patients with NB, indicating its role as an oncogene in NB. These findings revealed that LINC01296 promoted NB progression via binding with NCL.

Since LINC01296 is localized predominantly in the nucleus, the molecular mechanism of LINC01296 could also serve as a scaffold for recruiting diverse regulatory factors at a single locus. Therefore, we carried out ChIRP-seq analysis to explore DNA loci bound by LINC01296, and the results were confirmed by qPCR and qRT-PCR. Numerous validated, enriched genes of ChIRP-seq, such as BCL2, SOX11, BRD4, LMO3, and SMARCA1, have been reported to play critical roles in carcinogenesis.[23,25–27,40] The BCL2 family proteins regulate the mitochondrial or intrinsic apoptotic response, which is vital to suppress apoptosis in cancer cells.[23] BRD4 binds to the promoter and enhancer regions of oncogene MYCN and the promoter region of PHOX2B to activate their transcription in NB.[26] As a neural transcription factor, SOX11 is involved in embryonic neuron development, inflammation, and cancer pathology.[25] Several studies have demonstrated that SOX11 could exert oncogenic effects and function as a tumor suppressor, depending on the different kinds of tumors.[41] It has been reported that SOX11 could promote cell survival and tumor angiogenesis and inhibit B cell differentiation in mantle cell lymphoma.[42] In breast cancer, SOX11 is indispensable for the cell growth of endoplasmic reticulum (ER)-negative breast cancer cell lines and promotes EMT via Slug.[43,44] However, as a tumor suppressor, SOX11 represses cell growth, tumor invasion, and metastasis in gastric cancer.[45] In our study, we identified SOX11 as an oncogene in NB cells, enhancing cell proliferation and migration and inhibiting cell apoptosis, which is consistent with the results of Louwagie et al.[29,46] It has been reported that SOX11 KD showed decreased colony formation ability and G1-S cell-cycle arrest in NB cells, and SOX11 was co-expressed with MYCN.[46] Moreover, SOX11 regulates chromatin accessibility at active enhancers in adrenergic high-risk NB.[29] Furthermore, ectopic SOX11 expression could partially restore cell proliferation and migration, reduced by LINC01296 KD. We performed ChIP-qPCR and validated that NCL also bound the SOX11 promoter. These results suggested that the LINC01296-NCL complex could regulate SOX11 transcription, contributing to NB tumor aggressiveness.

In summary, the lncRNA LINC01296 promotes the progression of NB by transcriptional activating SOX11 by forming a complex with NCL. The LINC01296/NCL/SOX11 complex could serve as a prognostic biomarker. Considering the vital function of the LINC01296/NCL/SOX11 complex, it may also have the potential to be a promising therapeutic target for the treatment of NB.

MATERIALS AND METHODS

Cell lines

The SK-N-BE(2)C, CHLA20, HEK293T cell lines were obtained from the American Type Culture Collection (ATCC) (Manassas, VA), and the SK-N-AS, SK-N-SH, SK-N-BE(2), KP-N-NS, and IMR-32 cell

Figure 3. Activation of LINC01296 through the dCas9/SAM system enhances NB cell proliferation, migration and represses apoptosis *in vitro*

(A) qRT-PCR measured the efficiency of endogenous activation of LINC01296 through the dCas9/SAM system in SK-N-BE(2)C and SK-N-AS cells. (B) The CCK-8 assay revealed cell viability of NB cells after LINC01296 overexpression. Student's t test was performed on day 5 for 2 groups. (C and D) The colony formation assay revealed the clonogenic ability of NB cells with LINC01296 overexpression. (E and F) The EdU assay revealed an increased proportion of EdU^+ cells in the LINC01296 overexpressed NB cells. Scale bar, 100 μm. (G and H) Transwell assay revealed increased cell migration ability in the LINC01296 overexpressed NB cells after incubation for 24 h. Scale bar, 50 μm. HPF, high power field. (I and J) Flow cytometry analysis detected decreased apoptosis of NB cells with LINC01296 overexpression. (K) Western blot experiment measured the PARP, cleaved PARP, caspase-3, and cleaved caspase-3 protein expression in Scr and sgLINC01296 NB cells.

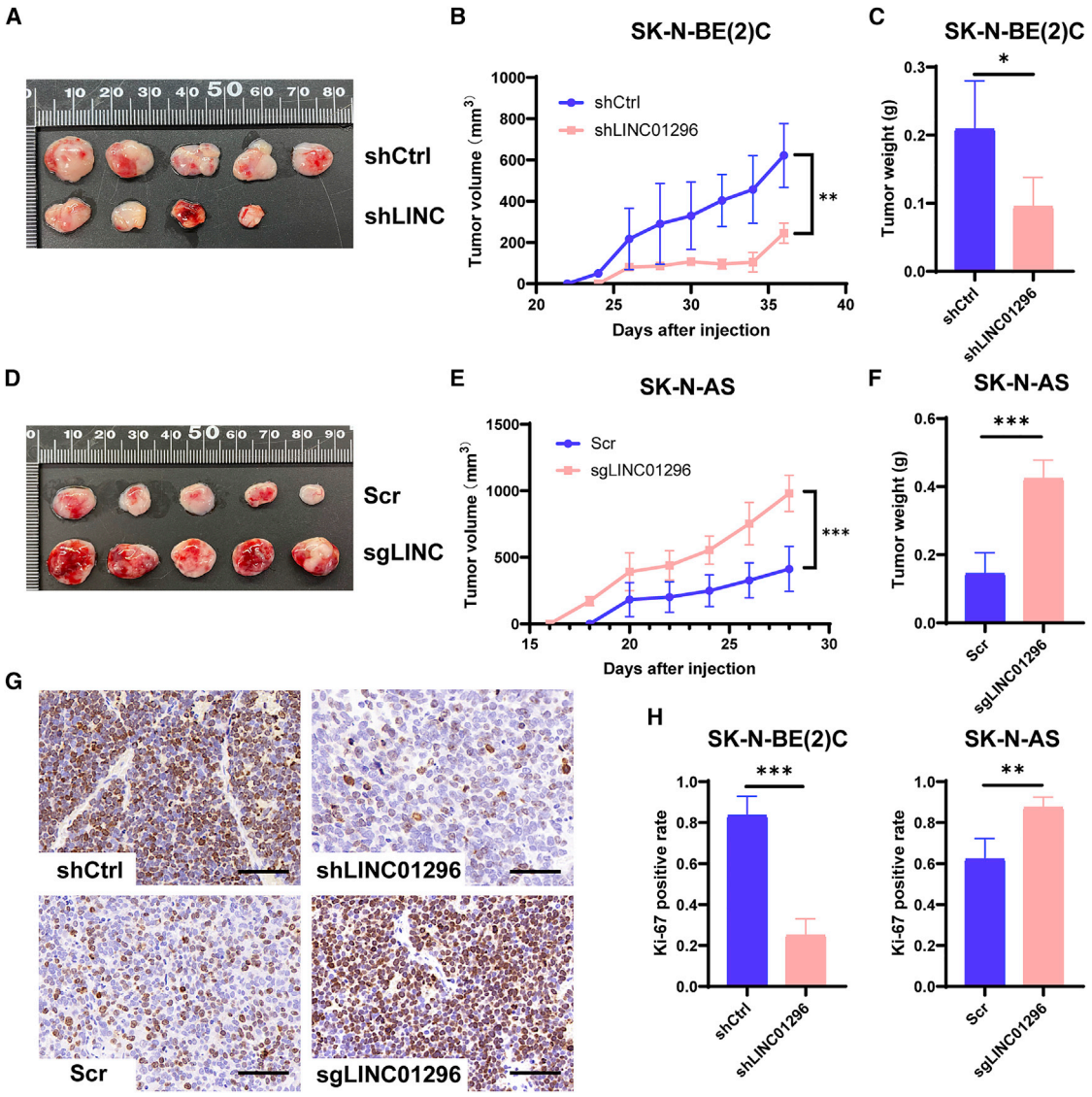

Figure 4. LINC01296 promotes tumor growth of NB *in vivo*

(A) Representative images of the xenograft tumors of SK-N-BE(2)C cells transfected with shCtrl, shLINC01296 at day 36 after injection. (B) Tumor volume was evaluated in SK-N-BE(2)C cells transfected with shCtrl, shLINC01296 every two days. Student's t-test was performed for two groups on day 36. (C) Tumor weight was measured in SK-N-BE(2)C cells transfected with shCtrl, shLINC01296 on day 36 after injection. (D) Representative images of the xenograft tumors of SK-N-AS cells transfected with Scr, sgLINC01296 on day 28 after injection. (E) Tumor volume was evaluated in SK-N-AS cells transfected with Scr, sgLINC01296 every 2 days. Student's t test was performed for 2 groups on day 28. (F) Tumor weight was measured in SK-N-AS cells transfected with Scr, sgLINC01296 on day 28 after injection. (G and H) Immunohistochemistry staining of Ki-67 in xenograft tumor samples (400×). Scale bar, 50 μm.

lines were purchased from the Type Culture Collection of the Chinese Academy of Sciences (Shanghai, China). All of the cell lines were tested routinely for mycoplasma contamination by PCR assay (Vazyme). SK-N-BE(2)C and SK-N-SH cell lines were cultured in F12/DMEM 1:1 (Gibco, Life Technologies) containing 10% fetal bovine serum (FBS) (Gibco, Life Technologies), 1% penicillin and streptomycin (Gibco, Life Technologies), and HEK293T and SK-N-AS were cultured in DMEM containing 10% FBS and 1% penicillin and streptomycin. All of the cell lines were cultured at 37°C in a humidified incubator with 5% CO_2.

Establishment of LINC01296 overexpression and stable KD cells

The open reading frame (ORF) of the SOX11 gene was cloned from the cDNA of the SH-SY5Y cell line and inserted into the pLVX-IRES-Hygro plasmid. In addition, the shRNA oligos of LINC01296 and NCL were annealed and cloned into the pLKO.1-puro vector.

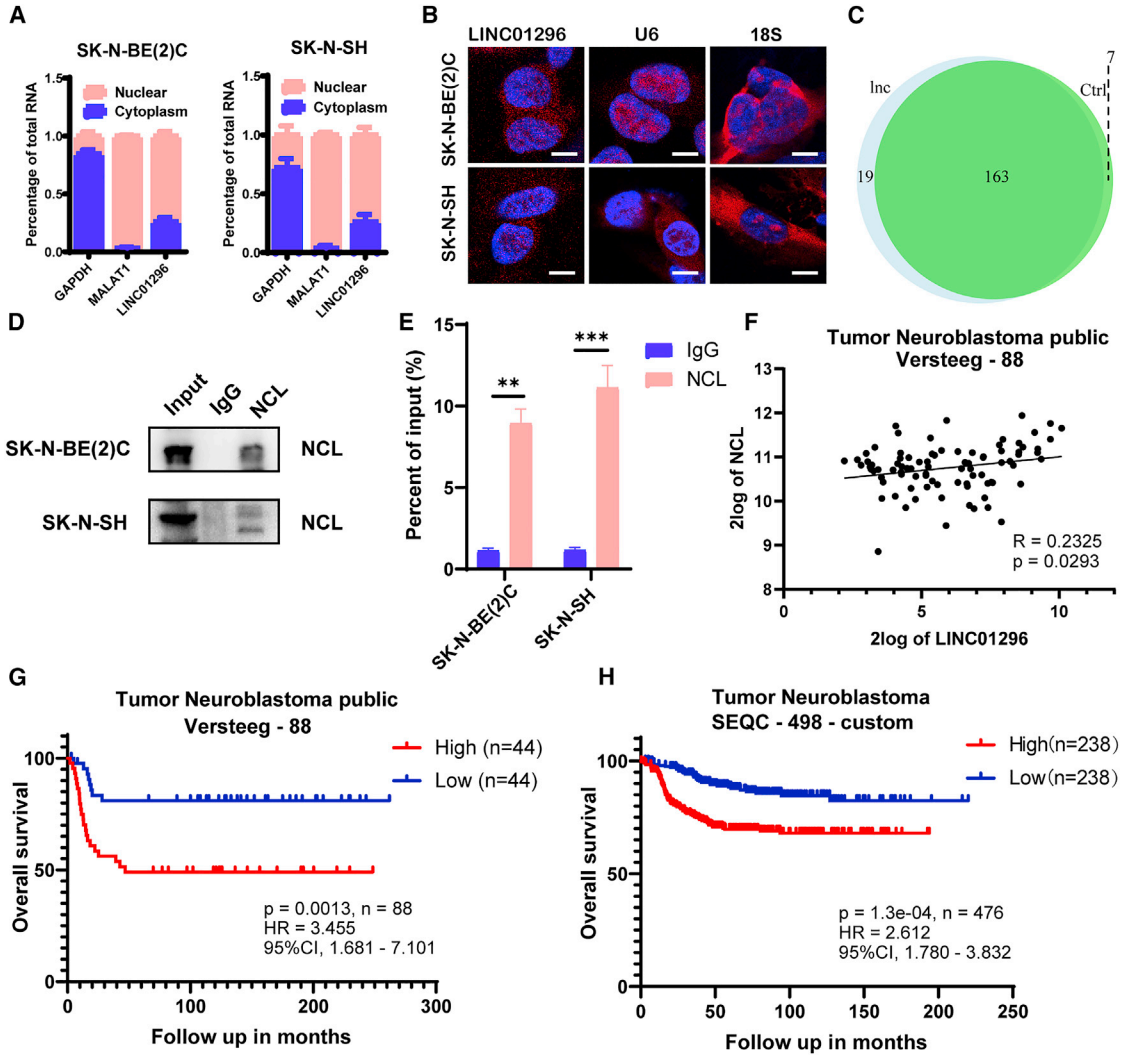

Figure 5. LINC01296 binds to NCL in NB cells

(A) Nuclear-cytoplasmic RNA extraction assay and qRT-PCR analysis for SK-N-BE(2)C and SK-N-SH cells showed LINC01296 was mainly located at the nucleus. GAPDH was used as the cytoplasmic internal control, and metastasis-associated lung adenocarcinoma transcript 1 (MALAT1) was used as the nuclear internal control. (B) RNA fluorescence *in situ* hybridization (RNA FISH) for SK-N-BE(2)C and SK-N-SH cells showed that LINC01296 was mainly located at the nucleus. The 18S probe was used as the cytoplasmic internal control, and the U6 probe was used as the nuclear internal control. Scale bar, 10 μm. (C) Venn diagram of LC-MS of chromatin isolation by RNA purification (ChIRP) showed 19 significant enriched proteins using LINC01296 probe compared to control probe. Lnc, LINC01296 probe; Ctrl, control probe. (D) Western blot confirmed the efficiency of immunoprecipitation (IP) of NCL antibody in RNA-binding protein IP (RIP) assay, and IgG was used as the negative control. (E) qRT-PCR analysis of RIP assay of SK-N-BE(2)C and SK-N-SH cells. IgG was used as the negative control. (F) The correlation between NCL mRNA expression and LINC01296 expression in clinical NB samples in the dataset containing 88 patients (Tumor Neuroblastoma public - Versteeg - 88, R2: Genomic Analysis and Visualization Platform). (G and H) Kaplan-Meier overall survival analysis of NCL mRNA expression in NB patients (n = 88, Tumor Neuroblastoma public – Versteeg – 88; n = 476, Tumor Neuroblastoma – SEQC – 498 – custom).

For 1 well of 6-well plates, lentivirus was produced by co-transfecting HEK293T cells with 2 μg lentivirus plasmids together with packaging plasmids 1.5 μg psPAX2 and 0.6 μg pMD2.G using 7 μL Lipofectamine 2000 reagent (Invitrogen). The virus was harvested through a 0.45-mm filter (Millipore) after 48 h of transfection. Collected lentivirus was used to directly infect cells with the addition of 8 mg/mL polybrene (Sigma-Aldrich) or stored in −80°C. Infected cells were selected with puromycin (Sigma-Aldrich) for 3–4 days at 1 μg/mL (SK-N-AS, SK-N-SH) or 3 μg/mL (SK-N-BE(2)C). LINC01296 activation in SK-N-BE(2)C and SK-N-AS cells was carried out through the dCas9-SAM gene activation system.[18] The SAM system involves 3 lentivirus plasmids, lenti_dCas9-VP64_Blast, lenti_MS2-p65-HSF1_Hygro, and lenti_sgRNA(MS2)_Puro. The lentiviruses of the 3 plasmids were used to infect SK-N-BE(2)C and SK-N-AS cells,

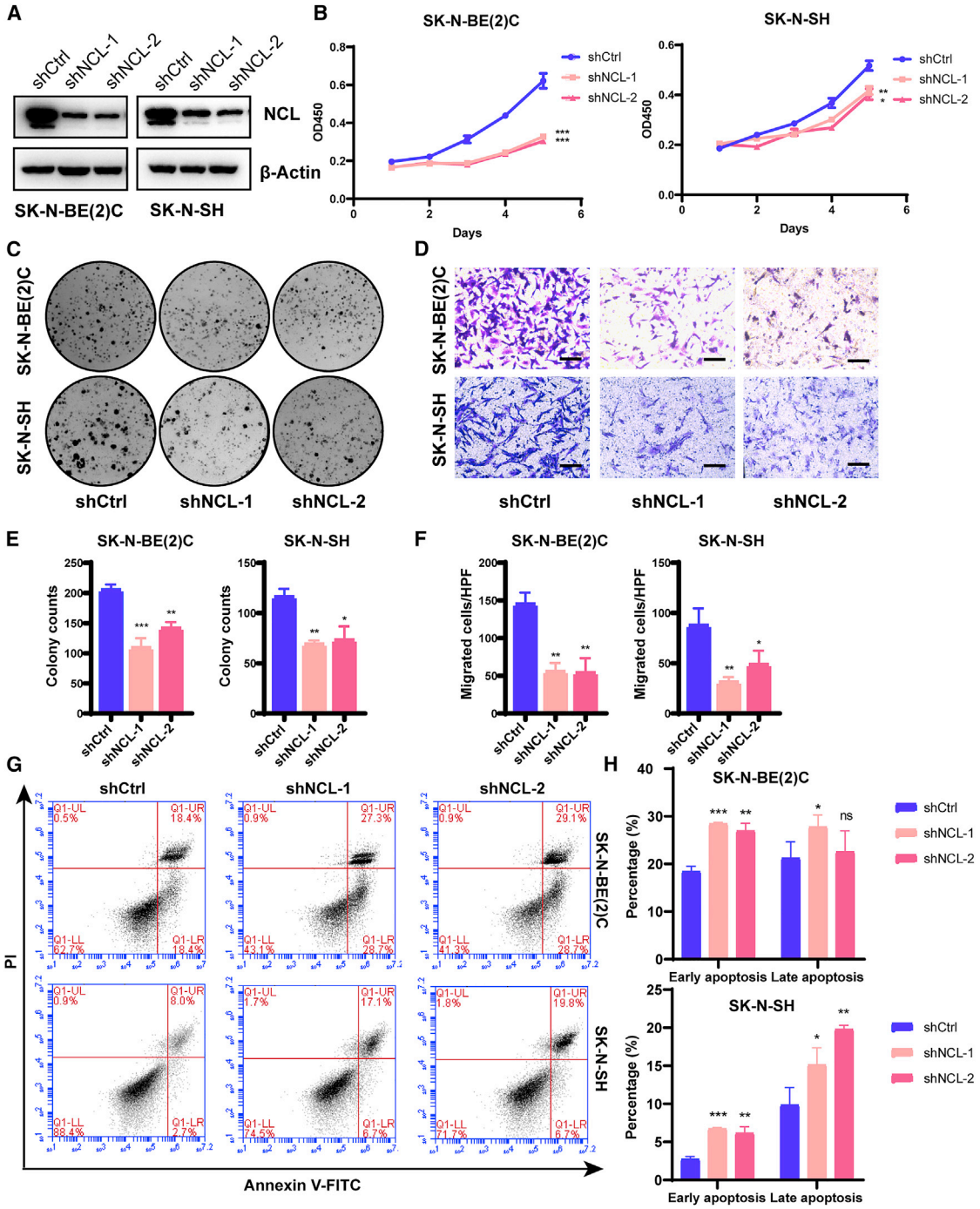

Figure 6. NCL acts as an oncogene and promotes NB progression

(A) Western blot measured the knockdown efficiency of NCL shRNAs in SK-N-BE(2)C and SK-N-SH cells. (B) CCK-8 assay showed reduced cell growth of NB cells after NCL knockdown. Student's t-test was performed on day 5 for each shNCL group compared to the shCtrl group. (C and E) The colony formation assay revealed the clonogenic ability of NB cells with NCL knockdown. (D and F) Transwell assay showed decreased cell migration ability in the LINC01296 knockdown cells after incubation for 24 h. Scale bar, 50 μm. (G and H) Flow cytometry analysis detected promoted apoptosis of NB cells silencing NCL. (E, F, and H) Student's t test was performed for each shNCL group compared to the shCtrl group.

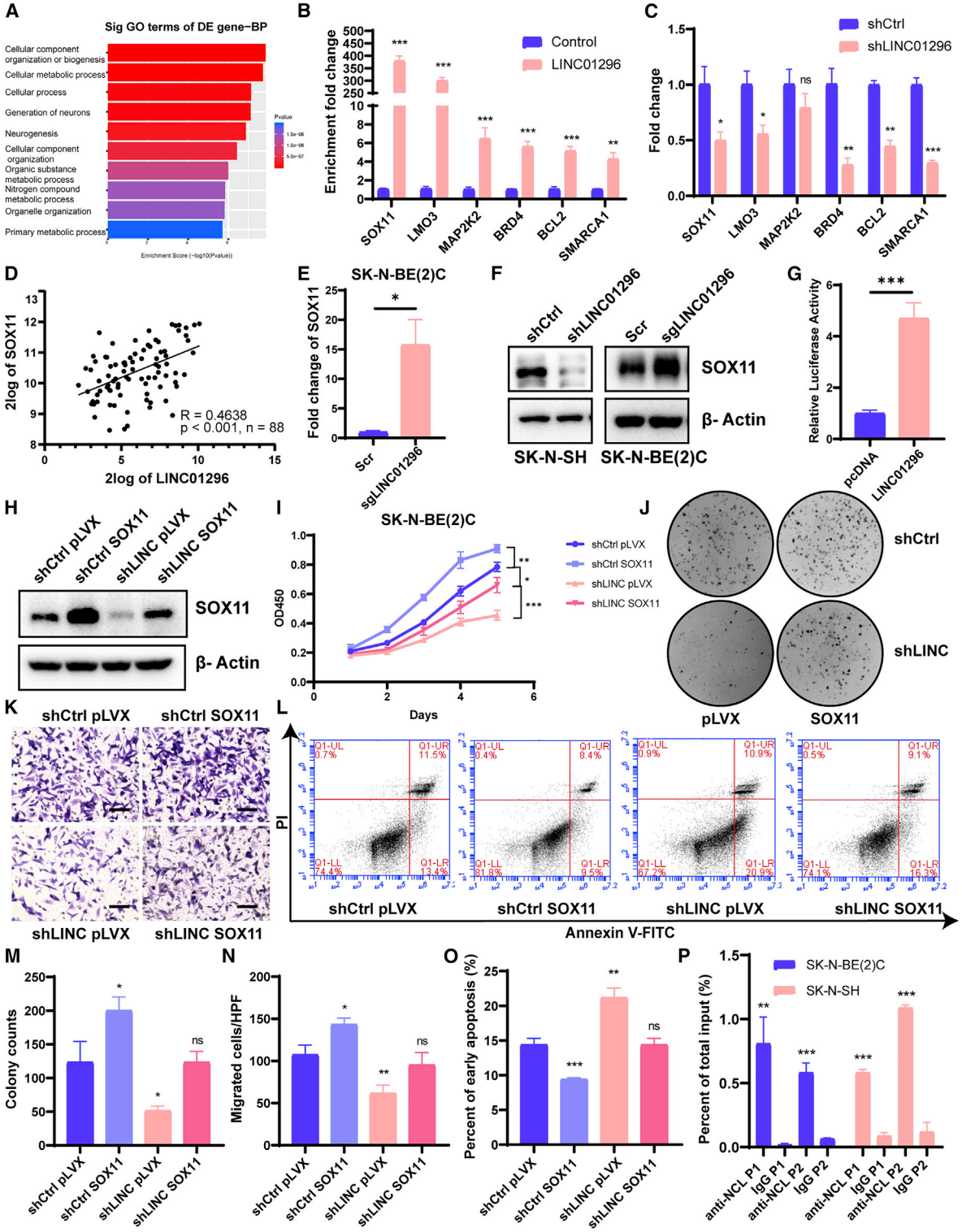

Figure 7. LINC01296-NCL promotes NB progression through transcriptionally activating SOX11 expression

(A) Gene Ontology (GO) analysis of differentially expressed genes in ChIRP-seq of SK-N-BE(2)C cells. (B) ChIRP-qPCR analysis detected the enrichment fold change of SOX11, LMO3, MAP2K2, BRD4, BCL2, and SMARCA1 genes in DNA pulled down by the LINC01296 probe compared to the control probe. (C) The qRT-PCR analysis

(legend continued on next page)

and cells were selected by antibiotics separately. Infected cells were selected with blasticidin (Sigma-Aldrich) for 1 week at 20 μg/mL and hygromycin for 1 week at 100 μg/mL. The oligos of shRNAs and sgRNAs used in this study are listed in Table S1.

RNA extraction and real-time qRT-PCR analysis

The total RNA of cells and tissues was extracted using TRIzol Reagent (Life Technologies) according to the manufacturer's protocol. RNA concentration and purity were measured by NanoDrop (Thermo Scientific), and each sample was adjusted to the same concentration at reverse transcription. cDNA was synthesized with the PrimeScript RT reagent Kit (TaKaRa) from 1,000 ng total RNA. The real-time qPCR analyses were conducted using ChamQ SYBR qPCR Master Mix (Vazyme) by the QuantStudio 7 Flex Real-Time PCR System (Applied Biosystems). Relative RNA expression was calculated by the ΔΔCt method with normalization to glyceraldehyde 3-phosphate dehydrogenase (GAPDH) mRNA. Primer sequences for qRT-PCR are listed in Table S2.

Western blot analysis

Cells were counted and cultured in 6-well plates with a confluence of 80%. Cells were rinsed with phosphate-buffered saline (PBS) twice and lysed with 120 μL/well M-PER Mammalian Protein Extraction Reagent (Thermo Scientific) containing protease and phosphatase inhibitor (Thermo Scientific). Cell lysates were scraped down and incubated on ice for 30 min, then centrifuged at 12,000 × *g* for 10 min, and the supernatants were transferred to clear tubes. After measuring the protein concentration using the bicinchoninic acid (BCA) protein assay (Pierce, Thermo Scientific), we denatured the proteins in SDS-PAGE (sodium dodecyl sulfate-polyacrylamide gel electrophoresis) Sample Loading Buffer (Biosharp) at 95°C for 10 min. Protein samples were separated by SDS-PAGE in polyacrylamide gels (EpiZyme) and transferred to nitrocellulose filter membranes (GE). Membranes were blocked in 5% non-fat milk/TBST (Tris-buffered saline with Tween) for 1 h at room temperature and incubated with primary antibody diluted in 5% non-fat milk/TBST overnight at 4°C. After washing with TBST, membranes were incubated with horseradish peroxidase-conjugated anti-rabbit or anti-mouse IgG (1:3,000, Cell Signaling Technology, #7074 and #7076) and analyzed by the FluorChem FC3 chemiluminescence system (Protein Simple). The antibodies used in immunoblot include SOX11 (1:2,000, Abcam, ab170916), NCL (1:2,000, Abcam, ab22758), caspase-3 (1:1,000, Cell Signaling Technology, #9662), cleaved caspase-3 (1:1,000, Cell Signaling Technology, #9664), PARP (1:1,000, Cell Signaling Technology, #9532), cleaved PARP (1:1,000, Cell Signaling Technology, #5625), and β-actin (1:10,000, Sigma-Aldrich, A3854).

Cell proliferation assay and cell migration assay

Cell proliferation was measured using the CCK-8 (Dojindo). Cells (5,000/well) were seeded into 96-well plates and were monitored daily for 5 consecutive days. The absorbance was read at 450 nm by a microplate reader (Bio-Tek). For the colony formation assay, a total of 2,000 SK-N-BE(2)C and SK-N-SH cells for shRNA and 1,000 SK-N-BE(2)C and SK-N-AS cells for the dCas9/SAM system were seeded into 6-well plates. After 2 weeks of culture, cells were fixed with 4% paraformaldehyde and stained with 0.1% crystal violet. According to the manufacturer's protocol, the cell proliferation ability was also detected by the EdU assay using the Cell-light EdU Apollo 567 *in vitro* kit (Ribobio). Following the manufacturer's instructions, the cell migration assay was carried out using 8.0-μm 24-well transwell chambers (Corning). A total of 5×10^4 SK-N-AS and SK-N-SH cells, 1.5×10^5 SK-N-BE(2)C cells for shRNA and 1×10^5 SK-N-BE(2)C cells for the dCas9/SAM system were resuspended in 100 μL FBS-free medium and seeded in each transwell; medium with 10% FBS was added to the wells of 24-well plates. After incubation for 24 h, cells in the bottom surface of membranes were fixed with 4% paraformaldehyde, stained with 0.1% crystal violet, and photographed in 3 independent fields per well using a Leica microscope.

Cell apoptosis analysis

The cells were collected 48 h after plating in 6-well plates. Cells were then washed and incubated with 5 μL annexin V-FITC (fluorescein isothiocyanate) and 5 μL PI (BD Pharmingen, 556547) for 15 min at room temperature and then resuspended in 400μL 1X binding buffer. The stained cells were detected and analyzed by a BD Accuri C6 flow cytometer.

RNA FISH

LINC01296 RNA FISH was performed using the Ribobio FISH Kit according to the manufacturer's protocol. U6 was used as the nuclear

measured the mRNA expression levels of SOX11, LMO3, MAP2K2, BRD4, BCL2, and SMARCA1 genes in shCtrl and shLINC01296 SK-N-BE(2)C cells. (D) The correlation between SOX11 mRNA expression and LINC01296 expression in clinical NB samples in the dataset containing 88 patients (Tumor Neuroblastoma public - Versteeg - 88, R2: Genomic Analysis and Visualization Platform). (E) The qRT-PCR analysis showed the upregulated mRNA expression level of SOX11 in sgLINC01296 SK-N-BE(2)C cells compared to Scr cells. (F) Western blot showed the reduced SOX11 protein expression in shLINC01296 SK-N-SH cells and elevated SOX11 protein expression in sgLINC01296 SK-N-BE(2)C cells. (G) Luciferase reporter assay was detected 48 h after the co-transfection of pcDNA3.1-LINC01296 and SOX11 promoter reporter vectors in 293T cells. (H) SOX11 protein expression level in shCtrl and shLINC01296 SK-N-BE(2)C cells with or without SOX11 overexpression assayed by immunoblotting. shCtrl pLVX, cells transfected with PLKO.1-shCtrl and pLVX-hygro plasmids; shCtrl SOX11, cells transfected with PLKO.1-shCtrl and pLVX-SOX11 plasmids; shLINC pLVX, cells transfected with PLKO.1-shLINC01296 and pLVX-hygro plasmids; shLINC pLVX and shLINC SOX11, cells transfected with PLKO.1-shLINC01296 and pLVX-SOX11 plasmids. (I) CCK-8 assay showed the cell growth rate of shCtrl and shLINC01296 SK-N-BE(2)C cells with or without SOX11 overexpression. Student's t test was performed on day 5 for shCtrl pLVX and shCtrl SOX11, shCtrl pLVX and shLINC SOX11, and shLINC pLVX and shLINC SOX11. (J and M) Colony formation assay of shCtrl and shLINC01296 SK-N-BE(2)C cells with or without SOX11 overexpression. (K and N) Transwell assay of shCtrl and shLINC01296 SK-N-BE(2)C cells with or without SOX11 overexpression after incubation for 24 h. Scale bar, 50 μm. (L and O) Flow cytometry analysis detected cell apoptosis of shCtrl and shLINC01296 SK-N-BE(2)C cells with or without SOX11 overexpression. (P) ChIP and qPCR assays showed NCL bound to SOX11 promoter in SK-N-BE(2)C and SK-N-SH cells. IgG, negative control; P1, primer 1; P2, Primer 2 (M–O). Student's t test was performed for shCtrl pLVX and each of the other groups, respectively.

control, and 18S was used as the cytoplasm control. All of the probes were labeled with Cy3, and the sequences of probes are listed in Table S3. The images were collected with a Leica confocal microscope.

Subcellular fraction extraction

Nuclear and cytoplasmic RNA extraction was conducted using NE-PER Nuclear and Cytoplasmic Extraction Reagents (Life Technologies) according to the manufacturer's protocol. After centrifuging, TRIzol was added to the pellet and supernatant for RNA extraction.

ChIRP

Biotin probes of LINC01296 used in ChIRP were designed using the online probe designer at singlemoleculefish.com. The cells were harvested, cross-linked, and conducted to the ChIRP experiment as described by Chu et al.[47] In addition, GO analysis and(KEGG analysis were carried out by the DAVID Functional Annotation web-based tool (http://david.ncifcrf.gov). The biotin probes used in ChIRP are listed in Table S4, and the primer sequences for ChIRP-qPCR are listed in Table S5.

RIP assay

RIP assays were conducted with the Magna RIP Kit (Millipore, #17–700) according to the manufacturer's instructions using 5 μg rabbit anti-NCL antibody (Abcam, ab22758) or 5 μg rabbit IgG (Millipore) for each immunoprecipitation. Protein isolated from the beads suspension during the last wash was collected to detect IP efficiency by western blotting. The immunoprecipitated RNAs were analyzed by qRT-PCR.

Luciferase reporter assay

The SOX11 promoter region and control sequence were cloned into the pGL4-basic vector. Full-length LINC01296 was cloned into the pcDNA 3.1 vector; 1×10^5 293T cells were plated in each well of 24-well plates. The next day, 250 ng SOX11 reporter vector, 250 ng LINC01296 ectopic expression vector, or the negative control vector were co-transfected with Lipofectamine 3000 reagent (Invitrogen). The Renilla plasmid (RL-SV40) was used as an internal control. Luciferase activity was detected 48 h after transfection using the Dual-Luciferase Reporter Assay System (Promega) with a luminometer (Bio-Tek). Firefly luciferase activity was normalized to Renilla luciferase activity. The data were represented as the percentage of luciferase activity in negative control cells.

Chromatin immunoprecipitation (ChIP) assay

SK-N-BE(2)C and SK-N-SH cell lines (1×10^7 cells per assay) were cross-linked with 1% formaldehyde (Sigma) at room temperature for 10 min and quenched in 125 mM glycine (Sigma) for 5 min. ChIP assays were carried out using the SimpleChIP Enzymatic Chromatin IP Kit (Cell Signaling Technology, #91820) according to the manufacturer's instructions. Chromatin fragments were immunoprecipitated with antibodies against normal rabbit IgG (5 μg, Cell Signaling Technology, #2729) and NCL (5μg, Abcam, ab22758). The qPCR primers used to amplify the promoter region are provided in Table S6.

In vivo assays

The procedures for the care and use of animal studies were approved by the ethics committee of Shanghai General Hospital. Six-week-old male BALB/c nude mice were used for the experiments. To carry out subcutaneous tumor growth assays *in vivo*, SK-N-BE(2)C and SK-N-AS cells (4×10^6 cells/mouse) were digested and injected in the left or right flank of nude mice (n = 5 per group) in 100 μL PBS. The tumor volumes and the animal weight were measured every 2 days. The tumor volumes were calculated according to the formula volume (mm^3) = length (mm) × width $(mm)^2/2$. The mice were killed by pentobarbital (250 mg/kg, intraperitoneal injection). Tumor samples were saved at −80°C or further embedded in paraffin for IHC.

IHC

The tissues embedded in paraffin were cut into 5-μm-thick sections. After dewaxing, antigen unmask, endogenous peroxidases were blocked with 3.5% H_2O_2 treatment for 15 min. Then, the nonspecific reaction was blocked with serum for 1 h. Next, the sections were incubated with Ki-67 (1:400, Cell Signaling Technology, #9027) antibodies overnight in a humidified chamber at 4°C. After washing, the sections were incubated with secondary antibody (Vector, biotinylated, 1:100) for 1 h at room temperature and then with ABC reagent (Vectastain ABC Kit) for 30 min at room temperature. Finally, DAB staining (Vector, DAB kit) was visualized by incubation for 2 min on the Leica microscope, and then counterstaining was performed. The percentages of positive cells were measured by Image Pro Plus 6.0.

Statistical analysis

The data analysis and graphical depiction of data were generated by GraphPad Prism 8 (GraphPad Software). Experimental data were represented as means ± standard deviations (SDs). Comparisons between groups were analyzed using a two-sided Student's t-test or one-way ANOVA. The correlation of genes was analyzed by Pearson's correlation. Kaplan-Meier curves of NB patients were analyzed by the log rank test. A p value of <0.05 was considered to be statistically significant. All of the results were reproduced in at least three independent experiments.

SUPPLEMENTAL INFORMATION

Supplemental information can be found online at https://doi.org/10.1016/j.omto.2022.02.007.

ACKNOWLEDGMENTS

This work was supported by grants from the Shanghai Municipal Key Clinical Specialty (no. shslczdzk05703), the Hengjie special support plan (2022, to K.L.), the Medical Innovation Research Special Project of Shanghai Science and Technology Innovation Action Plan (21Y11912200, to K.L.), the Research Project of Children's Hospital of Fudan University (EK112520180202, to K.L.), the Cyrus Tang Foundation, the National Natural Science Foundation of China (grant no. 82072782), the Shanghai Hospital Development Center (grant

nos. SHDC12018X22, SHDC2020CR2009A, and SHDC12020125, to K.D.), the Science Foundation of Shanghai (grant no. 19411966800, to K.D.), the Children's National Medical Center (grant nos. EK1125180112 and EK112520180301, to K.D.), the NSFC (82072571, to D.J.), the Shanghai Pujiang Scholar Program (19PJ1408500, to D.J.), the Experimental Animal Research Fund, Science, and Technology Commission of Shanghai Municipality (19140905600, to D.J.), the Shanghai Young Eastern Scholar Program (to D.J.), and the Natural Science Foundation of Shanghai (2022, to Z.W.).

AUTHOR CONTRIBUTIONS

K.L., K.D., D.J., and R.D. conceived and designed the work that led to the submission. J.W., Z.W., W.L., Q.H., H.Y., and W.Y. conducted the experiments. J.W. and Z.W. interpreted the results. J.W. drafted the manuscript. K.L., K.D., and D.J. approved the final version.

DECLARATION OF INTERESTS

The authors declare no competing interests.

REFERENCES

1. Louis, C.U., and Shohet, J.M. (2015). Neuroblastoma: molecular pathogenesis and therapy. Annu. Rev. Med. *66*, 49–63.
2. Shohet, J., and Foster, J. (2017). Neuroblastoma. BMJ *357*, j1863.
3. London, W.B., Castel, V., Monclair, T., Ambros, P.F., Pearson, A.D.J., Cohn, S.L., Berthold, F., Nakagawara, A., Ladenstein, R.L., Iehara, T., et al. (2011). Clinical and biologic features predictive of survival after relapse of neuroblastoma: a report from the International Neuroblastoma Risk Group project. J. Clin. Oncol. *29*, 3286–3292.
4. Pinto, N.R., Applebaum, M.A., Volchenboum, S.L., Matthay, K.K., London, W.B., Ambros, P.F., Nakagawara, A., Berthold, F., Schleiermacher, G., Park, J.R., et al. (2015). Advances in risk classification and treatment strategies for neuroblastoma. J. Clin. Oncol. *33*, 3008–3017.
5. Schmitt, A.M., and Chang, H.Y. (2016). Long noncoding RNAs in cancer pathways. Cancer Cell *29*, 452–463.
6. Slack, F.J., and Chinnaiyan, A.M. (2019). The role of non-coding RNAs in oncology. Cell *179*, 1033–1055.
7. Chi, Y., Wang, D., Wang, J., Yu, W., and Yang, J. (2019). Long non-coding RNA in the pathogenesis of cancers. Cells *8*, 1015.
8. Goodall, G.J., and Wickramasinghe, V.O. (2021). RNA in cancer. Nat. Rev. Cancer *21*, 22–36.
9. Young, S.W.S., Stenzel, M., and Jia-Lin, Y. (2016). Nanoparticle-siRNA: a potential cancer therapy? Crit. Rev. Oncol. Hematol. *98*, 159–169.
10. Bennett, C.F. (2019). Therapeutic antisense oligonucleotides are coming of age. Annu. Rev. Med. *70*, 307–321.
11. Xiu, B., Chi, Y., Liu, L., Chi, W., Zhang, Q., Chen, J., Guo, R., Si, J., Li, L., Xue, J., et al. (2019). LINC02273 drives breast cancer metastasis by epigenetically increasing AGR2 transcription. Mol. Cancer *18*, 187.
12. Liu, P.Y., Erriquez, D., Marshall, G.M., Tee, A.E., Polly, P., Wong, M., Liu, B., Bell, J.L., Zhang, X.D., Milazzo, G., et al. (2014). Effects of a novel long noncoding RNA, lncUSMycN, on N-Myc expression and neuroblastoma progression. J. Natl. Cancer Inst. *106*, dju113.
13. Nallasamy, P., Chava, S., Verma, S.S., Mishra, S., Gorantla, S., Coulter, D.W., Byrareddy, S.N., Batra, S.K., Gupta, S.C., and Challagundla, K.B. (2018). PD-L1, inflammation, non-coding RNAs, and neuroblastoma: immuno-oncology perspective. Semin. Cancer Biol. *52*, 53–65.
14. Mondal, T., Juvvuna, P.K., Kirkeby, A., Mitra, S., Kosalai, S.T., Traxler, L., Hertwig, F., Wernig-Zorc, S., Miranda, C., Deland, L., et al. (2018). Sense-antisense lncRNA pair encoded by locus 6p22.3 determines neuroblastoma susceptibility via the USP36-CHD7-SOX9 regulatory axis. Cancer Cell *33*, 417–434.e7.
15. Pandey Gaurav, K., Mitra, S., Subhash, S., Hertwig, F., Kanduri, M., Mishra, K., Fransson, S., Ganeshram, A., Mondal, T., Bandaru, S., et al. (2014). The risk-associated long noncoding RNA NBAT-1 controls neuroblastoma progression by regulating cell proliferation and neuronal differentiation. Cancer Cell *26*, 722–737.
16. Russell, M.R., Penikis, A., Oldridge, D.A., Alvarez-Dominguez, J.R., McDaniel, L., Diamond, M., Padovan, O., Raman, P., Li, Y., Wei, J.S., et al. (2015). CASC15-S is a tumor suppressor lncRNA at the 6p22 neuroblastoma susceptibility locus. Cancer Res. *75*, 3155–3166.
17. Wang, J., Wang, Z., Yao, W., Dong, K., Zheng, S., and Li, K. (2019). The association between lncRNA LINC01296 and the clinical characteristics in neuroblastoma. J. Pediatr. Surg. *54*, 2589–2594.
18. Konermann, S., Brigham, M.D., Trevino, A.E., Joung, J., Abudayyeh, O.O., Barcena, C., Hsu, P.D., Habib, N., Gootenberg, J.S., Nishimasu, H., et al. (2015). Genome-scale transcriptional activation by an engineered CRISPR-Cas9 complex. Nature *517*, 583–588.
19. Chen, L.-L. (2016). Linking long noncoding RNA localization and function. Trends Biochem. Sci. *41*, 761–772.
20. Wu, T., and Du, Y. (2017). LncRNAs: from basic research to medical application. Int. J. Biol. Sci. *13*, 295–307.
21. Jia, W., Yao, Z., Zhao, J., Guan, Q., and Gao, L. (2017). New perspectives of physiological and pathological functions of nucleolin (NCL). Life Sci. *186*, 1–10.
22. Ishimaru, D., Zuraw, L., Ramalingam, S., Sengupta, T.K., Bandyopadhyay, S., Reuben, A., Fernandes, D.J., and Spicer, E.K. (2010). Mechanism of regulation of bcl-2 mRNA by nucleolin and A+U-rich element-binding factor 1 (AUF1)*. J. Biol. Chem. *285*, 27182–27191.
23. Hata, A.N., Engelman, J.A., and Faber, A.C. (2015). The BCL2 family: key mediators of the apoptotic response to targeted anticancer therapeutics. Cancer Discov. *5*, 475–487.
24. Caunt, C.J., Sale, M.J., Smith, P.D., and Cook, S.J. (2015). MEK1 and MEK2 inhibitors and cancer therapy: the long and winding road. Nat. Rev. Cancer *15*, 577–592.
25. Tsang, S.M., Oliemuller, E., and Howard, B.A. (2020). Regulatory roles for SOX11 in development, stem cells and cancer. Semin. Cancer Biol. *67*, 3–11.
26. Puissant, A., Frumm, S.M., Alexe, G., Bassil, C.F., Qi, J., Chanthery, Y.H., Nekritz, E.A., Zeid, R., Gustafson, W.C., Greninger, P., et al. (2013). Targeting MYCN in neuroblastoma by BET bromodomain inhibition. Cancer Discov. *3*, 308.
27. Aoyama, M., Ozaki, T., Inuzuka, H., Tomotsune, D., Hirato, J., Okamoto, Y., Tokita, H., Ohira, M., and Nakagawara, A. (2005). LMO3 interacts with neuronal transcription factor, HEN2, and acts as an oncogene in neuroblastoma. Cancer Res. *65*, 4587.
28. Shi, J., Whyte, W.A., Zepeda-Mendoza, C.J., Milazzo, J.P., Shen, C., Roe, J.-S., Minder, J.L., Mercan, F., Wang, E., Eckersley-Maslin, M.A., et al. (2013). Role of SWI/SNF in acute leukemia maintenance and enhancer-mediated Myc regulation. Genes Dev. *27*, 2648–2662.
29. Decaesteker, B., Louwagie, A., Loontiens, S., De Vloed, F., Roels, J., Vanhauwaert, S., De Brouwer, S., Sanders, E., Denecker, G., D'haene, E., et al. (2020). SOX11 is a lineage-dependency factor and master epigenetic regulator in neuroblastoma. Preprint at bioRxiv, 2020.08.21.261131.
30. Qin, Q.-H., Yin, Z.-Q., Li, Y., Wang, B.-G., and Zhang, M.-F. (2018). Long intergenic noncoding RNA 01296 aggravates gastric cancer cells progress through miR-122/MMP-9. Biomed. Pharmacother. *97*, 450–457.
31. Jiang, M., Xiao, Y., Liu, D., Luo, N., Gao, Q., and Guan, Y. (2018). Overexpression of long noncoding RNA LINC01296 indicates an unfavorable prognosis and promotes tumorigenesis in breast cancer. Gene *675*, 217–224.
32. Liu, B., Pan, S., Xiao, Y., Liu, Q., Xu, J., and Jia, L. (2018). LINC01296/miR-26a/GALNT3 axis contributes to colorectal cancer progression by regulating O-glycosylated MUC1 via PI3K/AKT pathway. J. Exp. Clin. Cancer Res. *37*, 316.
33. Hu, X., Duan, L., Liu, H., and Zhang, L. (2019). Long noncoding RNA LINC01296 induces non-small cell lung cancer growth and progression through sponging miR-5095. Am. J. Transl. Res. *11*, 895–903.

34. Chen, C., He, W., Huang, J., Wang, B., Li, H., Cai, Q., Su, F., Bi, J., Liu, H., Zhang, B., et al. (2018). LNMAT1 promotes lymphatic metastasis of bladder cancer via CCL2 dependent macrophage recruitment. Nat. Commun. *9*, 3826.

35. Zhu, T., An, S., Choy, M.-T., Zhou, J., Wu, S., Liu, S., Liu, B., Yao, Z., Zhu, X., Wu, J., et al. (2019). LncRNA DUXAP9-206 directly binds with Cbl-b to augment EGFR signaling and promotes non-small cell lung cancer progression. J. Cell. Mol. Med. *23*, 1852–1864.

36. Statello, L., Guo, C.-J., Chen, L.-L., and Huarte, M. (2021). Gene regulation by long non-coding RNAs and its biological functions. Nat. Rev. Mol. Cell Biol. *22*, 96–118.

37. Liang, P., Jiang, B., Lv, C., Huang, X., Sun, L., Zhang, P., and Huang, X. (2013). The expression and proangiogenic effect of nucleolin during the recovery of heat-denatured HUVECs. Biochim. Biophys. Acta Gen. Subj. *1830*, 4500–4512.

38. Wang, X., Yu, H., Sun, W., Kong, J., Zhang, L., Tang, J., Wang, J., Xu, E., Lai, M., and Zhang, H. (2018). The long non-coding RNA CYTOR drives colorectal cancer progression by interacting with NCL and Sam68. Mol. Cancer *17*, 110.

39. Wang, F., Zhou, S., Qi, D., Xiang, S.-H., Wong, E.T., Wang, X., Fonkem, E., Hsieh, T.-C., Yang, J., Kirmani, B., et al. (2019). Nucleolin is a functional binding protein for salinomycin in neuroblastoma stem cells. J. Am. Chem. Soc. *141*, 3613–3622.

40. Weischenfeldt, J., Dubash, T., Drainas, A.P., Mardin, B.R., Chen, Y., Stütz, A.M., Waszak, S.M., Bosco, G., Halvorsen, A.R., Raeder, B., et al. (2017). Pan-cancer analysis of somatic copy-number alterations implicates IRS4 and IGF2 in enhancer hijacking. Nat. Genet. *49*, 65–74.

41. Yang, Z., Jiang, S., Lu, C., Ji, T., Yang, W., Li, T., Lv, J., Hu, W., Yang, Y., and Jin, Z. (2019). SOX11: friend or foe in tumor prevention and carcinogenesis? Ther. Adv. Med. Oncol. *11*, 1758835919853449.

42. Palomero, J., Vegliante, M.C., Rodríguez, M.L., Eguileor, Á., Castellano, G., Planas-Rigol, E., Jares, P., Ribera-Cortada, I., Cid, M.C., Campo, E., et al. (2014). SOX11 promotes tumor angiogenesis through transcriptional regulation of PDGFA in mantle cell lymphoma. Blood *124*, 2235–2247.

43. Liu, D.-T., Peng-Zhao, Han, J.-Y., Lin, F.-Z., Bu, X.-M., and Xu, Q.-X. (2014). Clinical and prognostic significance of SOX11 in breast cancer. Asian Pac. J. Cancer Prev. *15*, 5483–5486.

44. Xiao, Y., Xie, Q., Qin, Q., Liang, Y., Lin, H., and Zeng, D. (2020). Upregulation of SOX11 enhances tamoxifen resistance and promotes epithelial-to-mesenchymal transition via slug in MCF-7 breast cancer cells. J. Cell. Physiol. *235*, 7295–7308.

45. Qu, Y., Zhou, C., Zhang, J., Cai, Q., Li, J., Du, T., Zhu, Z., Cui, X., and Liu, B. (2014). The metastasis suppressor SOX11 is an independent prognostic factor for improved survival in gastric cancer. Int. J. Oncol. *44*, 1512–1520.

46. Louwagie, A. (2019). Abstract 2596: SOX11 is a key epigenetic regulatorin the adrenergic MYCN amplified neuroblastomas. Cancer Res. *79*, 2596.

47. Chu, C., Quinn, J., and Chang, H.Y. (2012). Chromatin isolation by RNA purification (ChIRP). J. Vis. Exp. *61*, 3912.